SHEAR BEHAVIOUR IN SLENDER REINFORCED CONCRETE BEAMS WITHOUT STIRRUPS

Hasini C. Weerasinghe [1], Michele Win Tai Mak [2], Janet M. Lees [3]

1. PhD Candidate, Department of Engineering, University of Cambridge, United Kingdom
2. Research Associate, Department of Engineering, University of Cambridge, United Kingdom
3. Professor, Department of Engineering, University of Cambridge, United Kingdom

Abstract

Many analytical tools for the prediction of the shear capacity of reinforced concrete beams do not explicitly predict the crack kinematics that reflect the actual cracking behaviour. As a result, most models require experimentally measured crack patterns and kinematics as input parameters. Hence the crack analysis is a post-assessment technique for shear failures exhibited in laboratory specimens. A significant challenge in the development of a priori critical shear crack analysis is that the critical shear crack shape is known to be unpredictable. There is thus an important need for approaches that reliably and accurately predict the shape of a critical shear crack in slender reinforced concrete beams. Experiments on shear-critical concrete beams without transverse reinforcement were undertaken to investigate the influence of the span to depth ratio and longitudinal reinforcement ratio on the crack shape at failure. Digital image correlation was used to map the dominant crack which was then modelled mathematically using curve fitting tools. The crack shapes were normalised with respect to the beam depth to compare the results for different span to depth ratios. It was found that the beams with longitudinal reinforcement ratios between 0.84% and 1.50% had similar critical crack shapes but the crack shape in the beam with 2.35% reinforcement differed. In the latter case, the dominant crack intersected with the longitudinal steel closer to the beam support leading to a shorter delamination crack and higher ultimate capacity. The initial findings of the study provide a basis for the development of crack-based predictive tools for the shear behaviour of slender reinforced concrete beams without transverse reinforcement.

Keywords: *Shear crack geometry, delamination crack, crack kinematics*

INTRODUCTION

The shear behaviour of reinforced concrete (RC) beams has been the subject of extensive research for over 100 years [1]. Nevertheless, there remains a lack of understanding in the underpinning fundamental shear mechanisms. The complexity of the problem can be partly attributed to the large number of parameters that affect the shear response of reinforced concrete. Several theories are based on the notion that the ultimate capacity of reinforced concrete in shear is related to the characteristics of a discrete crack. These theories often have an empirical or semi-empirical basis derived from experimental observations. The resulting analytical formulations can require a number of simplifications, presenting significant challenges, especially in relation to the characteristics of dominant shear cracks and their measured kinematics [2]. With recent advances in photogrammetry, Digital Image Correlation (DIC) has become a useful tool to measure crack kinematics in experimental investigations [3], [4]. However, while this approach improves the analysis of concrete shear cracks, it has primarily been applied as a post-assessment technique for shear failures exhibited in laboratory experiments. Therefore, the next step is to exploit DIC insights to develop methods for the forward prediction of shear failures.

Evaluating the shear behaviour of reinforced concrete beams with accuracy and precision requires knowledge of the shape of the critical shear crack. Once the shape has been determined, the crack kinematics could be estimated, and the contributions of the associated shear transfer mechanisms can be calculated. Since the crack kinematics are highly dependent on the crack shape, investigating the parameters which influence the crack shape is of scientific interest.

BACKGROUND

The importance of the shape of the Critical Shear Crack (CSC) can be inferred from the relevant literature. Campana et. al. [4] performed a comparison of the relative contributions of shear transfer mechanisms (namely uncracked concrete, aggregate interlock and dowel action) in cases where the critical crack had different curvatures. Their study highlighted that the governing shear transfer mechanisms can differ due to changes in the crack geometry [4]. In their investigation, steeper curved cracks exhibited a higher aggregate interlock contribution than flatter linear cracks [4]. Therefore, if the beam parameters that lead to particular crack shapes can be isolated, the crack formation can potentially be manipulated e.g., through the use of mixes with a higher proportion of aggregates.

Kani's early work [5] included studies on size effects in concrete. A comparison of geometrically similar beams without transverse reinforcement with shear span-to-depth a/d = 4.0 was carried out to investigate the dependence of the shear resistance on the total depth of a beam. All the relevant parameters, including the shear span-to-depth (a/d = 4.0), remained constant except for the total depth which was varied between 305 mm and 1,219 mm. Although differences were observed in the overall cracking pattern, the shape of CSC remained similar despite the change in size.

Bentz et. al. [6] carried out an experimental investigation on beams without transverse reinforcement and with varying depths, shear span-to-depth (a/d) ratios ranging from 3 to 3.6 and longitudinal reinforcement ratios ρ_l ranging from 0.328% to 1.730%. Their results indicated that the shape of the CSC did not depend on ρ_l. Campana et. al. [4] tested beams with a/d = 3.5, with different concrete properties and ρ_l. In their beams without stirrups, the CSC was similar in shape and location regardless of the varying parameters. However, a change in CSC shape was observed in their tests on beams with shear reinforcement and different longitudinal reinforcement ratios.

Huber et. al. [7] carried out an experimental programme on beams without shear reinforcement with a/d = 3.04. Their results showed no correlation between the shape or location of the CSC and parameters such as member size, concrete type, and cross-section. Nevertheless, when the crack patterns from different specimens are compared, similarities can be identified in the characteristics and shape of the CSC.

The results from the existing literature, therefore, suggest that the shape of the CSC in slender beams without shear reinforcement may not have a strong dependence upon the proportion of longitudinal steel and the geometrical parameters. This hypothesis is inconclusive and further investigations are necessary. The objective of the current work is to ascertain if it is possible to reliably predict the shape of the CSC in beams without transverse reinforcement. This advance would facilitate the development of kinematic models based on the shape of the CSC rather than linear approximations, potentially leading to improved predictions of the shear capacity of RC beams.

EXPERIMENTAL PROGRAMME

An experimental programme on shear-critical RC beams without shear links was carried out to investigate the effect of geometrical and material properties on the shape of the CSC. A total of 4 specimens were tested in 3-point bending. The cross-section geometry, shear span-to-depth ratio, longitudinal reinforcement and concrete composition were varied.

All the specimens were prismatic beams and were grouped into two series, named A and B respectively. In the naming convention adopted in this study, the first letter A or B corresponds to the relevant mix composition (see Table 1) and cross-section geometry (see Figure 1). The subsequent number indicates the a/d ratio, and the last number corresponds to the longitudinal reinforcement ratio expressed as a percentage.

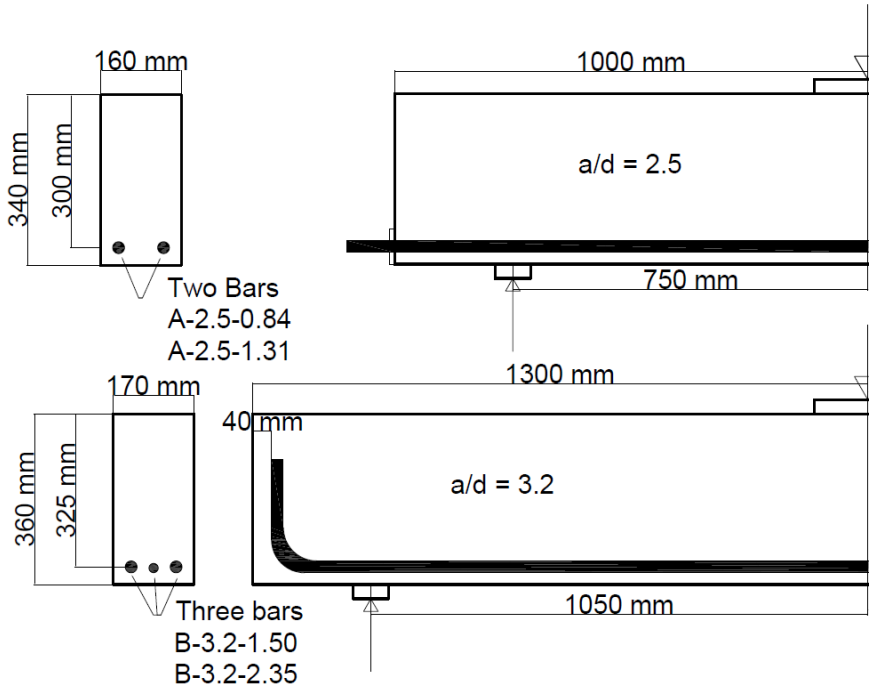

Figure 1-Test setup and specimen details

Specimens in series A had a rectangular cross-section of 160×340 mm, an overall length of 2,000 mm and a shear span of 750 mm, resulting in a span-to-depth ratio of 2.5. The bottom reinforcement consisted of two high strength deformed steel bars, anchored using square steel plates welded at each end. In specimen A-2.5-0.84, the reinforcement bars were 2H16 (ρ_l = 0.84%) with a cover of 24 mm, whereas in specimen A-2.5-1.31, the bars were 2H20 (ρ_l = 1.31%) with a cover of 20 mm. The size of the loading plate at the point of load application was 225×25 mm and the size of the support plate was 150×25 mm. Specimens in series B has a cross-section of 170×360 mm, an overall length of 2,600 mm and a shear span of 1,050 mm with *a/d* = 3.2. The longitudinal reinforcement consisted of 2H20 and 1H16 (ρ_l = 1.50%) in specimen B-3.2-1.50; 2H25 and 1H20 (ρ_l = 2.35%) in specimen B-3.2-2.35. In series B, the reinforcement had a cover of 25 mm, and the bars were anchored with a 90-degree bend. The geometrical characteristics of the specimens are shown in Figure 1.

The concrete used in both series was an Ordinary Portland Cement with no admixtures. Mix A was a high-strength concrete with a target cube strength of 50 MPa and a maximum aggregate size d_{max} = 10 mm, whereas Mix B was a normal strength concrete with a target strength of 40 MPa and d_{max} = 20 mm. The compositions of the two mixes are summarised in Table 1.

Table 1-Concrete mix composition

	Mix A	Mix B
Target strength	50 MPa	40 MPa
Cement Type	CEM I 52.5N	CEM II 32.5N
Water	220	205
Cement	700	445
Fine aggregate	855	700
Coarse aggregate (4 – 10 mm)	550	-
Coarse aggregate (4 – 20 mm)	-	1,010

The specimens were load tested 28 days after casting in 3-point bending with a symmetric arrangement. The bottom simple supports allowed for the rotation of the beam ends on either side of the specimens. The load was applied at the midspan on the top of the beam with a hydraulic actuator. The loading protocol consisted of three stages. Initially, the test was conducted in load control, at a rate of 0.5 kN/min. The load was increased up to 20 kN as a preload and then reduced back to zero. As the second step, the load was subsequently increased up to 50 kN. At this point (step three) the test was changed and controlled by the displacement, at a rate of 0.02 mm/min until failure. The vertical displacements of the specimens at critical points were measured with wire gauges.

Test Results

Table 2 compares the shear capacities of all four beam specimens. All the specimens failed in shear. The failure was sudden due to the formation of a critical shear crack that extended through the shear span. Specimens A-2.5-0.84 and A-2.5-1.31 failed at a shear load of 60.9 kN and 65.8 kN respectively and exhibited a similar critical shear crack pattern at almost the same location in the middle of the shear span. Hence the crack patterns and the failure loads were similar even though ρ_l differed. Specimen B-3.2-1.50 failed at a shear force of 65.0 kN whereas B-3.2-2.35 failed at 75.5 kN. The shape of the CSC in B-3.2-1.50 had a longer delamination branch along the level of the reinforcement than in B-3.2-2.35. Relatively speaking, the shear crack pattern in B-3.2-2.35 was shifted more towards the support and therefore was associated with a shorter length over which delamination occurred. Photographs of the specimens after failure are shown in Figure 2, where the positions and the shapes of the CSCs can be observed.

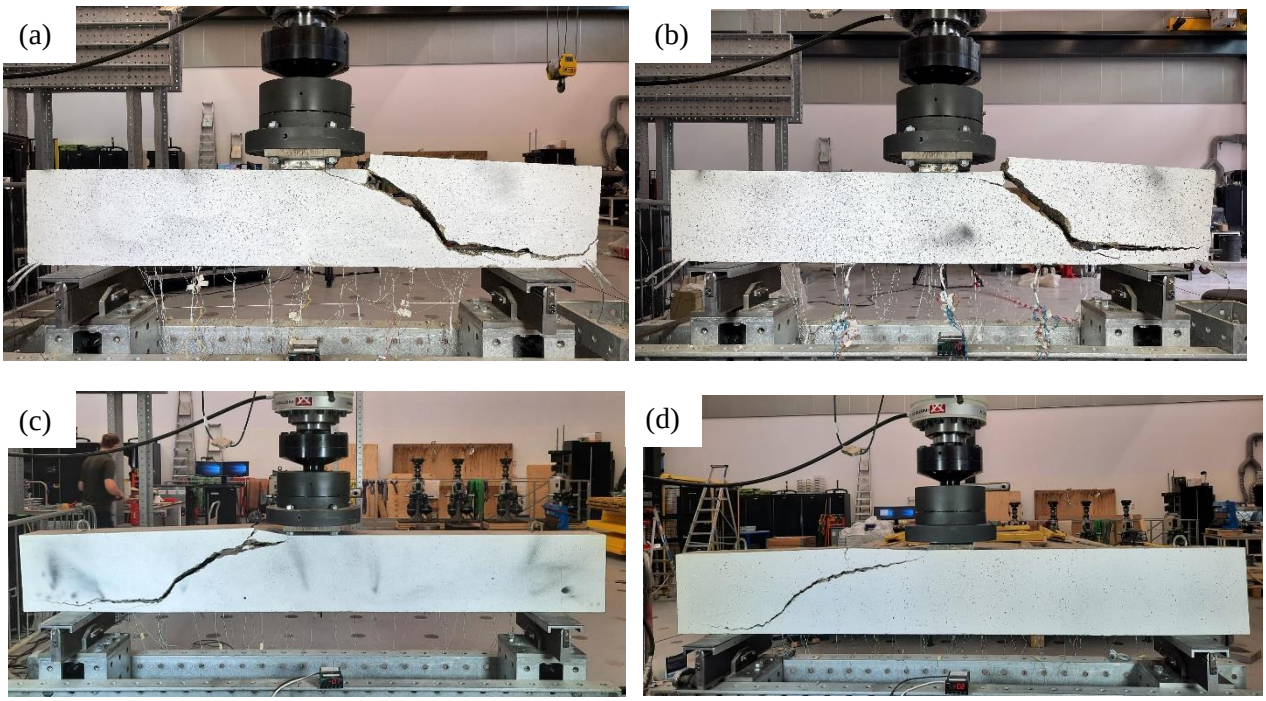

Figure 2 - Specimens at failure (a) A-2.5-0.84 (b) A-2.5-1.31 (c) B-3.2-1.50 (d) B-3.2-2.35

Table 2-Material properties and strength of tested specimens

Specimen	Concrete cube compressive strength f_c (MPa)	Span/depth ratio (*a/d*)	Longitudinal reinforcement ratio $\rho_l = A_s/bd$	Rebar configuration (mm)	$V_{max} = P/2$ (kN)
A-2.5-0.84	44.6	2.5	0.84%	2H16	60.9
A-2.5-1.31	51.9	2.5	1.31 %	2H20	65.8
B-3.2-1.50	35.87	3.2	1.5 %	2H20, 1H16	65.0
B-3.2-2.35	46.05	3.2	2.35 %	2H25, 1H20	75.5

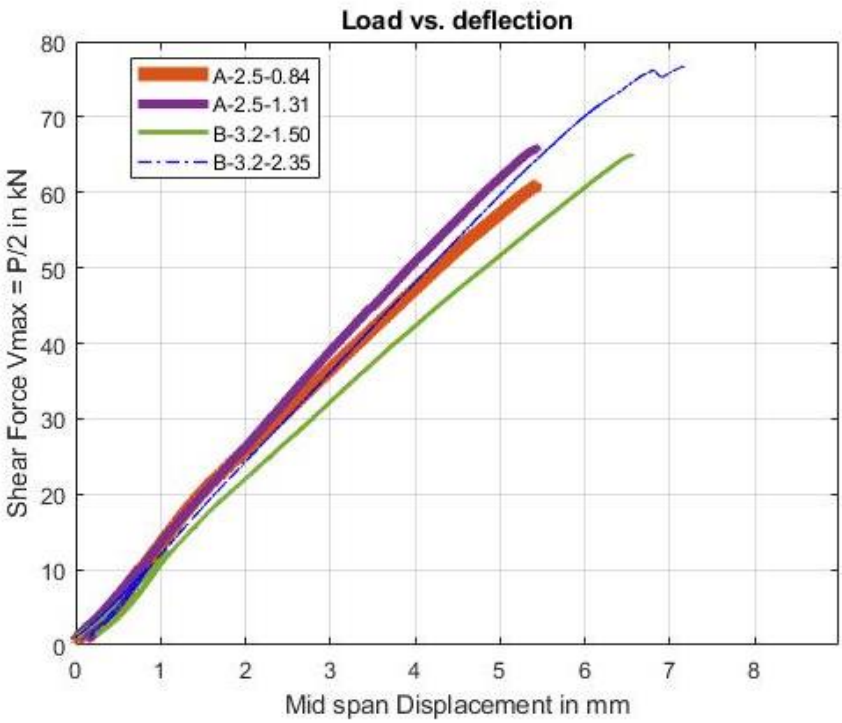

Figure 3 - Load-deflection curves for beams A-2.5-0.84, A-2.5-1.31, B-3.2-1.50 and B-3.2-2.35

The plots in Figure 3 show the load-deflection curves for all four specimens. The horizontal axis corresponds to the vertical displacement measured at midspan whereas the vertical axis is the nominal shear force, calculated as half the applied central point load ($P_{central}$). All four specimens exhibited a similar behaviour with an initial linear segment up to a displacement of 1.5 mm for series A and 1 mm for series B. Thereafter there was a reduction in stiffness, but the behaviour remained fairly linear until the beams failed in a brittle manner. However, the difference in response between the two series, B beams is much bigger than that observed in the series A tests even though the proportional difference in ρ_l is 1.56 times higher in both series. This observation suggests that there is possibly an advantageous strength gain when the CSC is located more towards the support since that is the main difference between the cracks that occurred in B-3.2-1.50 and B-3.2-2.35.

Best-fit polynomials

A mathematical representation of the shape of the critical shear crack is required to allow the forward prediction of shear capacity. Since linear approximations so far have not yielded the actual shear behaviour in slender RC beams, existing curved crack geometries such as Carpinteri's exponential curve [8] and Campana et. al.'s spline approximation [4] were considered. However, the inability of an exponential curve to capture a horizontal delamination crack and the dependency of a spline

approximation on measured crack patterns became potential issues [4], [8]. Therefore, MATLAB Curve Fitting Toolbox was applied to investigate the best-fit curves for the actual crack coordinates observed in the experiments. The goodness of the fit was analysed according to R-square and Root Mean Square Error (RMSE) values. It was ensured that the best-fit curve had $R^2 > 0.99$ and the lowest RMSE when arriving at a polynomial relationship with a degree of 5 (see Figure 4) [9].

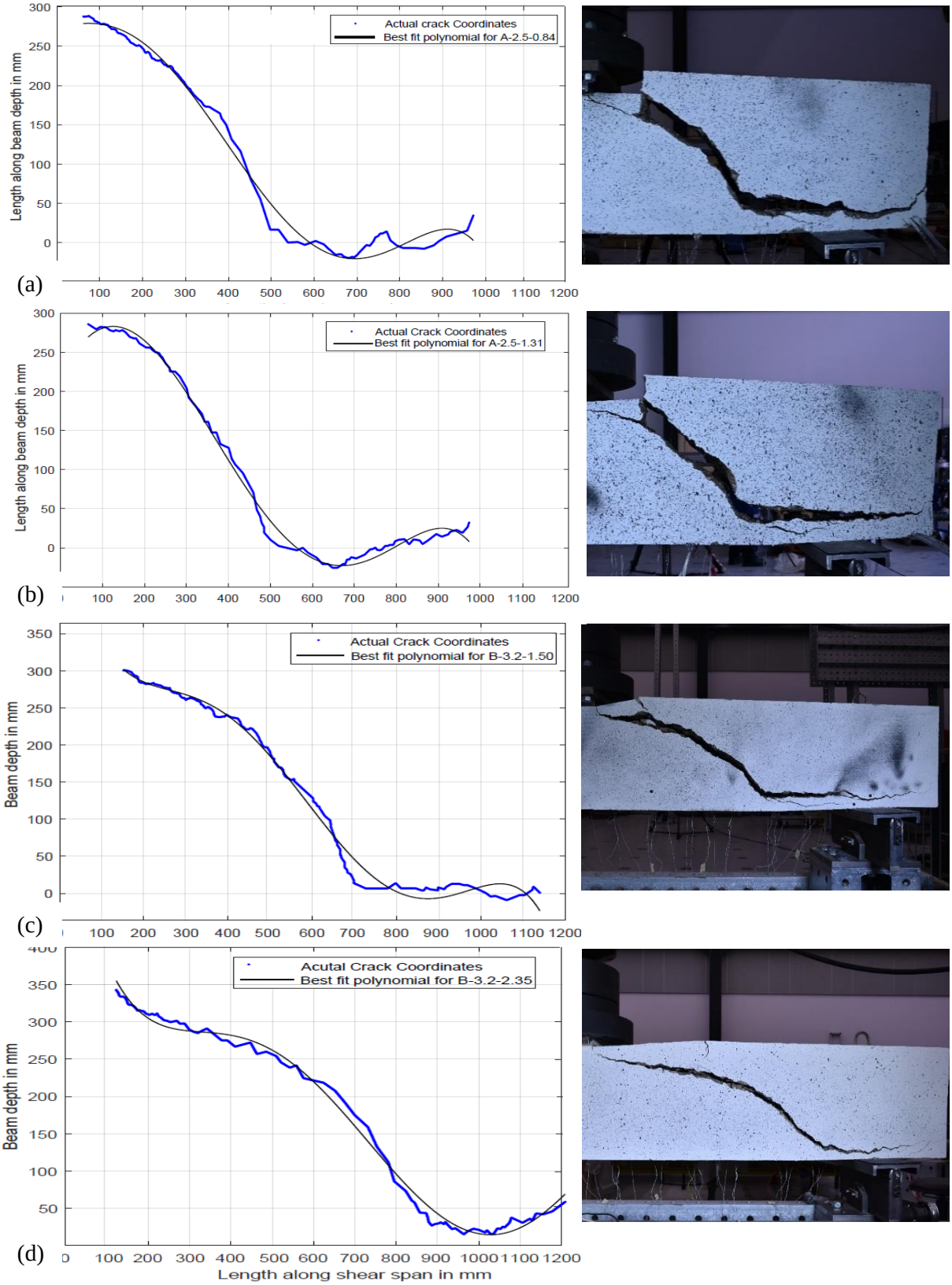

Figure 4 - Best-fit polynomials for (a) A-2.5-0.84 (b) A-2.5-1.31 (c) B-3.2-1.50 (d) B-3.2-2.35

The choice of the best curve was not only based on the statistical metrics of best-fit, but also on the crack geometry at the compression zone and the level of the longitudinal tensile reinforcement. The resulting curves for the region that excludes the delamination cracks are shown in Figure5(a). However, to compare the polynomials associated with the different beam cross-sections and shear spans used here, the location and the size of the crack were also normalised with respect to beam depth to check the similarity in the curve shapes. The normalised curves are presented in Figure 5(b).

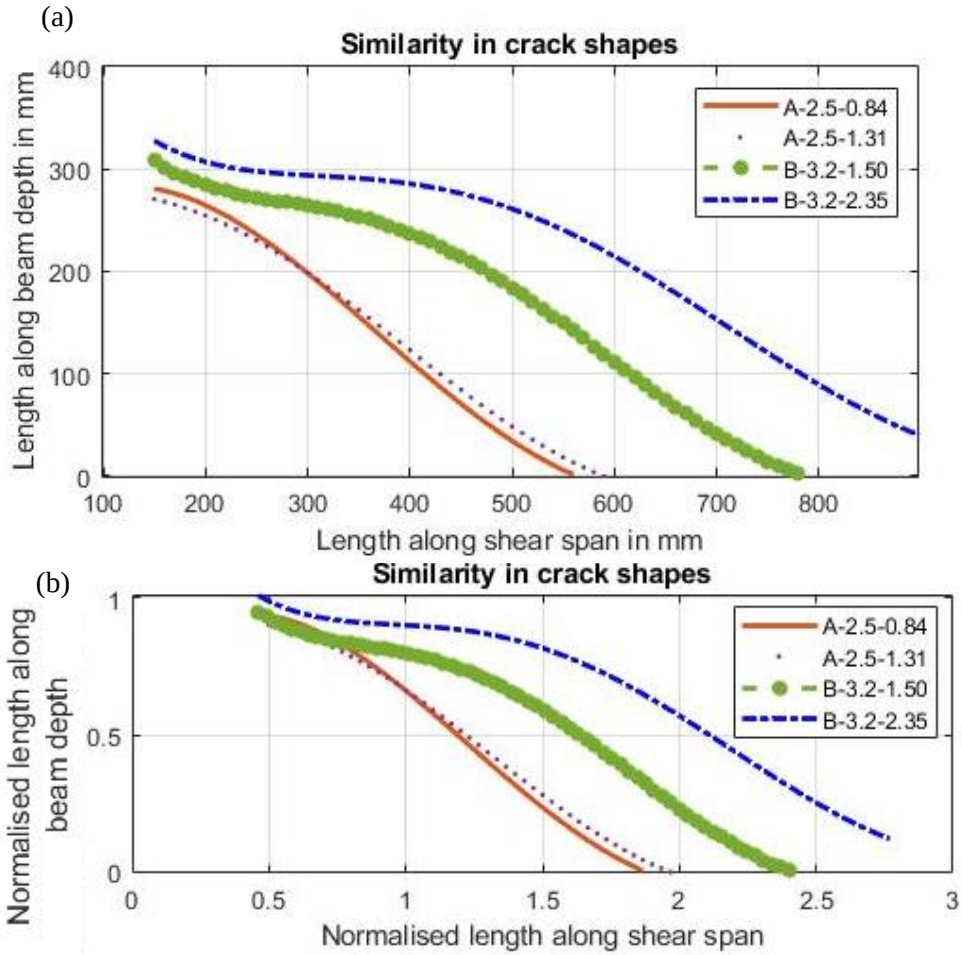

Figure 5- (a) Critical shear crack shapes (b) normalised crack shapes

From Figure 5(a), it can be seen that the curves for series A are almost the same shape. In both series A beams, the CSC is located at the middle of the shear span and therefore the raw and normalized (Figure 5(b)) curves lie over each other. However, the curves for series B have slightly different curvatures towards the intersection with the longitudinal steel (although noting too the deviation between the best fit and the actual crack in this region in B-3.2-1.50) but the shape of the crack segment near the crack tip is similar. In general, the curve for B-3.2-2.35 seems flatter than the crack shapes in the other three specimens. When the curve for B-3.2-1.50 is compared with curves for series A, the change towards the crack tip reflects the way the crack propagated towards the compression zone, but the crack shapes are in good agreement over the rest of the crack length. Therefore, this similarity check suggests that, for the parameters studied here, the shape of the CSC in the slender RC beams without shear reinforcement could potentially be predicted using a common base critical crack shape.

CONCLUSIONS

Four shear-critical slender reinforced concrete beams without shear reinforcement were tested in 3-point bending to explore the shape of the Critical Shear Crack (CSC). The parameters under

investigation were the type of concrete, span to depth ratio and the longitudinal reinforcement ratio ρ_l. The crack shapes were mathematically represented using curve fitting tools to map the crack shape. It was found that a 5th-degree polynomial generally captured the crack shapes of the slender RC beams without shear reinforcement. With the exception of a beam with a higher percentage of longitudinal reinforcement (2.35%), the normalised shapes of the CSC were similar. Further investigations are required to generalise these initial findings.

ACKNOWLEDGEMENTS

The first author would like to gratefully acknowledge the support of the Cambridge Commonwealth, European and International Trust for the HRH The Prince of Wales Commonwealth Scholarship for PhD study at the University of Cambridge. The second and third authors are grateful for the financial support received from the United Kingdom Engineering and Physical Science Research Council (EPSRC) via the Fellowship 'Tailored Reinforced Concrete Infrastructure: boosting the Innate Response to Chemical and Mechanical Threats'[EP/N017668/1]. The assistance of the technical staff in the University of Cambridge Structures Research Laboratory was invaluable when conducting the experimental work presented here.

REFERENCES

[1] M. P. Collins, E. C. Bentz, E. G. Sherwood, and L. Xie, "An adequate theory for the shear strength of reinforced concrete structures," *Mag. Concr. Res.*, vol. 60, no. 9, pp. 635–650, 2008, doi: 10.1680/macr.2008.60.9.635.

[2] H. P. J. Taylor, "Fundamental Behaviour in Bending and Shear of Reinforced Concrete. (Unpublished Doctoral Thesis, University of London)," 1971.

[3] T. Huber, P. Huber, and J. Kollegger, "Influence of aggregate interlock on the shear resistance of reinforced concrete beams without stirrups," *Eng. Struct.*, vol. 186, no. January, pp. 26–42, 2019, doi: 10.1016/j.engstruct.2019.01.074.

[4] S. Campana, M. F. Ruiz, A. Anastasi, and A. Muttoni, "Analysis of shear-transfer actions on one-way RC members based on measured cracking pattern and failure kinematics," *Mag. Concr. Res.*, vol. 65, no. 6, pp. 386–404, 2013, doi: 10.1680/macr.12.00142.

[5] G. N. J. Kani, "How safe are our large reinforced concrete beams?," *ACI J. Proc.*, vol. 64, no. 3, 1967, doi: 10.14359/7549.

[6] A. S. Lubell, E. C. Bentz, and M. P. Collins, "Influence of longitudinal reinforcement on one-way shear in slabs and wide beams," *J. Struct. Eng.*, vol. 135, no. 1, pp. 78–87, 2009, doi: 10.1061/(ASCE)0733-9445(2009)135:1(78).

[7] P. Huber, T. Huber, and J. Kollegger, "Investigation of the shear behavior of RC beams on the basis of measured crack kinematics," *Eng. Struct.*, vol. 113, pp. 41–58, 2016, doi: 10.1016/j.engstruct.2016.01.025.

[8] A. Carpinteri, J. R. Carmona, and G. Ventura, "Propagation of flexural and shear cracks through reinforced concrete beams by the bridged crack model," *Mag. Concr. Res.*, vol. 59, no. 10, pp. 743–756, 2007, doi: 10.1680/macr.2007.59.10.743.

[9] H. C. Weerasinghe and J. M. Lees, "The effect of shear crack geometry on aggregate interlock action in reinforced concrete," in *Concrete Structures: New Trends for Eco-efficiency and Performance, Proceedings of the fib Symposium 2021, Lisbon, Portugal.*, 2021, pp. 1730–1737.